OPEN ACCESS

Global Journal of Research in Agriculture & Life Sciences
ISSN: 2583-4576 (Online)
Volume 06 | Issue 06 | Nov.-Dec. | 2026
Journal homepage: https://gjrpublication.com/gjrals/

Research Article

A chemo-informatics Strategy to Understand the Mode of Binding Interaction, Mechanism of Free Radical Scavenging, and Pharmacokinetic Profile of some Antioxidant Agents

*Umma Muhammad [1] and Muhammad Tukur Ibrahim [2]

[1]Department of Science Laboratory Technology, School of Technology, Kano State Polytechnic, Kano State, Nigeria.
[2]Department of Chemistry, Faculty of Physical Sciences, Ahmadu Bello University, Zaria, Nigeria.

DOI: 10.5281/zenodo.24158303 **Submission Date: 30 Sept. 2026 | Published Date: 12 Nov. 2026**

***Corresponding author: Umma Muhammad**
Department of Science Laboratory Technology, School of Technology, Kano State Polytechnic, Kano State, Nigeria.
E-mail.: ummahammad@gmail.com

Abstract

Excessive reactive oxygen and nitrogen species cause oxidative stress, leading to a variety of chronic illnesses, highlighting the need for new antioxidants. This study applied a chemoinformatics approach to eleven 1-naphthol derivatives to elucidate their binding mode to human peroxiredoxin 5 (PDB ID: 1HD2), free-radical scavenging mechanisms, and pharmacokinetic profiles. Ligands were optimized at the B3LYP/6-311G(d) level and docked using Molegro Virtual Docker. Thermodynamic parameters for the hydrogen-atom transfer (HAT), single-electron transfer–proton transfer (SET-PT), and sequential proton-loss electron transfer (SPLET) pathways were computed, together with global reactivity descriptors. ADME-Tox and drug-likeness properties were predicted with Swiss ADME and pk CSM. Compounds 8, 6, and 11 exhibited the strongest binding affinities (−88.98, −86.20, and −84.72 kcal mol^{-1}, respectively) and formed key interactions with ALA90, ARG86, and LEU96. Bond-dissociation enthalpies (291.8–304.6 kJ mol^{-1}) indicated that the HAT mechanism is thermodynamically preferred over SET-PT and SPLET. Compound 11 displayed the narrowest HOMO–LUMO gap and lowest chemical hardness. All three candidates complied with Lipinski's rule of five, showed high intestinal absorption (> 91 %), and lacked predicted hepatotoxicity. These results identify selected 1-naphthol derivatives as promising antioxidant leads that combine target engagement, favorable radical-scavenging thermodynamics, and acceptable pharmacokinetic properties.

Keywords: *Chemoinformatics; Molecular docking; Peroxiredoxin 5; Free-radical scavenging; Hydrogen-atom transfer; DFT; Pharmacokinetics; 1-Naphthol derivatives.*

Introduction

Oxidative stress is a pathophysiological condition characterized by an imbalance between the systemic generation of reactive oxygen species (ROS) and the systemic antioxidant defenses against their concentration, resulting in damage to cells or tissues (Jomova *et al.*, 2023). These are most often reactive oxygen species (ROS) which include hydroxyl radical ($OH^{\bullet}$), superoxide anion radical ($O_2^{\bullet-}$) and hydroperoxyl radical ($HOO^{\bullet}$)), and reactive nitrogen species (RNS) such as nitric oxide radical ($NO^{\bullet}$) and nitrogen dioxide radical ($NO_2^{\bullet}$) that can be excessively produced as a result of external consequences (like polluted air with high levels of smog, exposure to X-rays, cigarette smoking and heavy metals) or internal consequences (Hamid *et al*., 2010; Lone *et al*., 2013; Kabel, 2014; Oke *et al*., 2019; Sharifi-Rad *et al*., 2020). Excessive free-radical accumulation can induce oxidative modification of proteins, lipids, and nucleic acids. If the resulting damage overwhelms cellular antioxidant and repair mechanisms, severe and potentially irreversible cellular injury or cell death may occur (Chandimali *et al.*, 2025).

Free radicals are species of molecules that comprise an unpaired electron. They are well known and serve as both useful and harmful species to the human system. They are formed when cells generate energy from food and oxygen, and also when exposed to microbial infections, extensive exercise, or pollutants/toxins such as cigarette smoke, alcohol, ionizing and UV radiation, pesticides, and ozone (Wu *et al.*, 2004). At physiological concentrations, they are involved in critical cellular functions such as cell signaling and defense against invading pathogens. Their activity is regulated by enzymatic

@ 2026 | PUBLISHED BY GJR PUBLICATION, INDIA

and nonenzymatic antioxidants to maintain the balance of the whole redox system and to prevent further oxidative damage (Patlevič *et al.*, 2016). Free radicals are also involved in physiological signaling and host defense mechanisms. However, excessive generation of free radicals induces oxidative damage to nucleic acids, lipids, and proteins. Therefore, oxidative stress is believed to be a contributing factor in the development and/or progression of diseases such as cardiovascular disease, diabetes, rheumatoid arthritis, neurodegenerative disorders, age-related diseases, and cancer (Reddy, 2023).

Antioxidants are compounds that inhibit, delay, or arrest the oxidation of biological substrates by deterring or trapping free radicals, donating electrons or protons, chelating transition metals, and scavenging molecules that promote endogenous antioxidant activities. In addition to inhibiting, some antioxidants can directly react with free radicals, preventing the production of oxygen free radicals and the chain reactions that cause widespread damage to these critical biomolecules before they occur. Natural antioxidants are found in foods, including fruits, vegetables, nuts, legumes, whole-grain cereals, tea, spices such as thyme, pepper, n-meg, dark chocolate, and antioxidant vitamins such as ascorbic acid (in fruit and vegetables) (Sotler *et al.*, 2019).

This work aimed at employing a chemoinformatics Strategy to understand the mode of binding interaction, mechanism of free radical scavenging, and pharmacokinetic profile of some 1-naphthol derivatives as potential antioxidant agents.

Methods

Antioxidant compounds (dataset)

A dataset consisting of eleven (11) 1-naphthol derivatives as potential antioxidant agents was obtained from the literature of Erdogan and co-workers for this investigation (Erdoğan *et al.*, 2021).

2D-molecular geometry sketching and best 3D-molecular geometry search

The 2D-molecular geometry of the obtained 1-naphthol derivatives (dataset) was drafted and sketched using the professional version 16.0 of ChemDraw (Mills, 2006). The best 3D-molecular geometry search for all the investigated eleven (11) 1-naphthol derivatives in this research were gotten at the MMFF with DFT at B3LYP/6-311G(d) theory level, respectively (Kohn *et al.*, 1996; Pawara *et al.*, 2021). Table 1 shows the 2D molecular structure of the investigated eleven (11) 1-naphthol derivatives.

Table 1. The 2D molecular structure of the investigated 1-naphthol derivatives

Entry ID	2D molecular geometry	Entry ID	2D molecular geometry
1	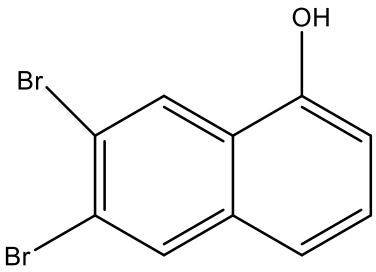	7	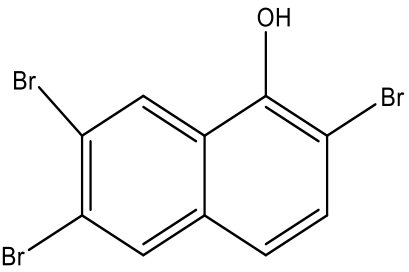
2	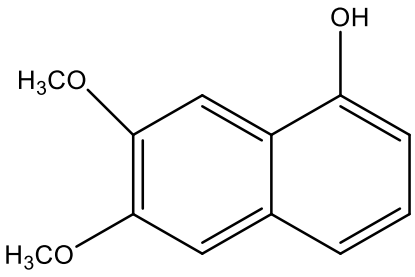	8	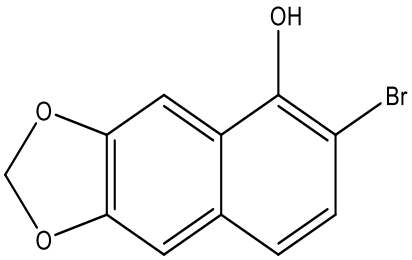

@ 2026 | PUBLISHED BY GJR PUBLICATION, INDIA

3	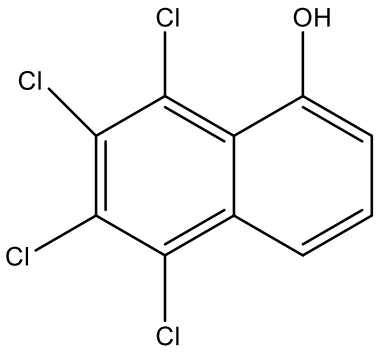	9	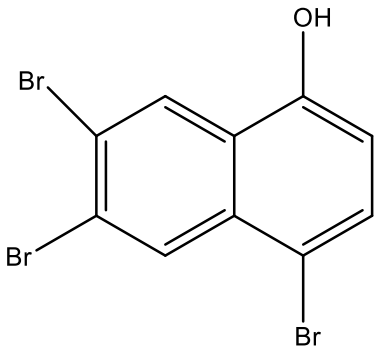
4	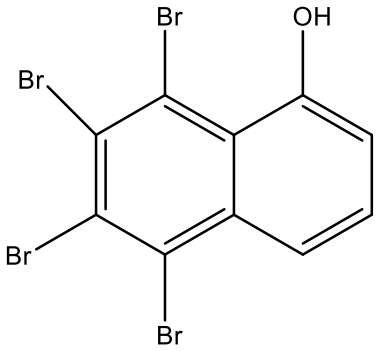	10	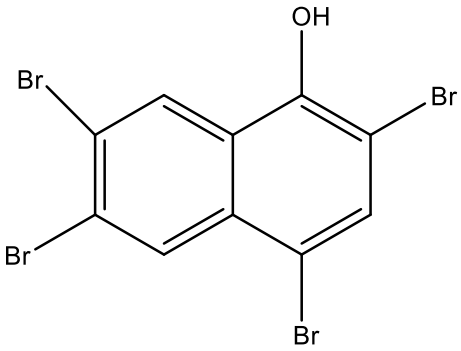
5	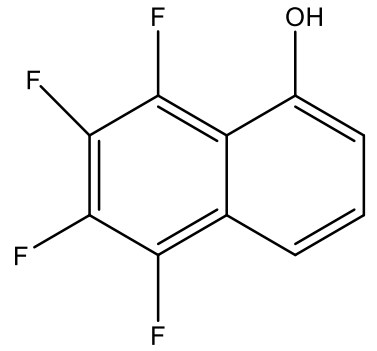	11	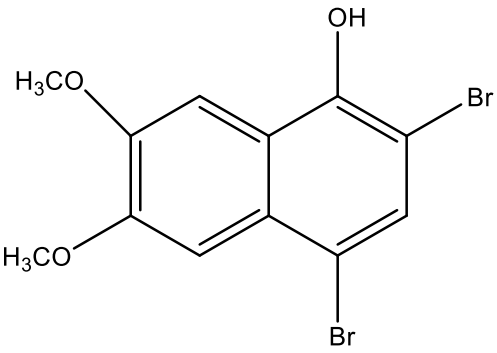
6	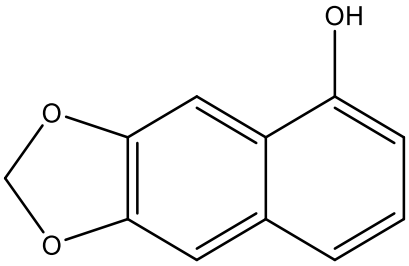		

Molecular docking-based virtual screening

1-naphthol derivatives and human peroxiredoxin 5 enzyme optimizations

The eleven (11) sets of 3D molecular geometries of the 1-naphthol derivatives obtained were prepared using the default settings of Molegro virtual docker (MVD) by selecting "if missing" for the restrictions used by the software for the preparation of ligands (Ghamali *et al.*, 2016; Ibrahim *et al.*, 2020).

The server of the RCSB protein data bank database at (https://www.rcsb.org/) was used as the basic source where the human peroxiredoxin 5 target enzyme with PDB entry code 1HD2 was retrieved (Dincel *et al.*, 2020). Furthermore, the hydrogens and the missing atoms on the human peroxiredoxin 5 target enzyme were complemented before it was optimized by removing the heteroatoms, water molecules, and co-factors with the 2021 version of BioVIA Discovery Studio Visualizer, respectively (Ibrahim *et al.*, 2025).

@ 2026 | PUBLISHED BY GJR PUBLICATION, INDIA

Docking procedure and its validation

The procedure of the molecular docking was performed by selecting the energy total (kcal/mole) as the scoring function. The dimensions of the grid box to define the pose cavities existing at the active site of the protein were set at seventeen Ångström units (17Å). Afterwards, for all other calculation procedures, the default settings were conserved and sustained (Abdullahi *et al.*, 2020).

The protocol validation of the molecular docking was executed by docking compound 8 into the binding pose of the human peroxiredoxin 5 target enzyme, and the root mean square deviation (RMSD) value of the again docked compound in the active site of the human peroxiredoxin 5 target enzyme was noted as 0.234Å, respectively.

Investigation of the Free Radical Scavenging Mechanisms of the Best Three Compounds

Antioxidants mechanism of free radical scavenging has been studied using numerous mechanisms (Khodja *et al.*, 2020). But the most widely reported ones in the literature are: hydrogen atom transfer (HAT), sequential electron transfer-proton transfer (SET-PT) and sequential proton loss electron transfer (SPLET), respectively. Density functional theory (DFT) calculations with Gaussian 09 software using the B3LYP/6-311G(d) basis set were used for all calculations to predict the HAT, SET-PT and SPLET mechanisms (Khodja *et al.*, 2020). The use of the B3LYP/6-311G(d) basis set was reported by many researchers (Amić *et al.*, 2018; Khodja *et al.*, 2020). The thermodynamic descriptors (BDE, IE, PDE, PA, ETE) of the antioxidant mechanisms were calculated using the equations reported in the literature (Amić *et al.*, 2017). The computed enthalpies of the hydrogen ($H^{\cdot}$) are -0.499897 Hartree (-1312.92kJ/mol), electron (e^{-}) is -.001198Hartree (3.15kJ/mol), and proton (H^{+}) are 0.002363 Hartree (6.20kJ/mol), all in the gas phase, were taken from the literature and converted from Hartree to kJ/mol, respectively (Amić *et al.*, 2018; Bartmess, 1994; Bizarro *et al.*, 1999; Klein *et al.*, 2009; Parker, 1992).

Reactivity and quantum chemical descriptors compilation

Reactivity parameters (E_{HOMO}, E_{LUMO} and energy band gap) and the quantum chemical descriptors were compiled using the B3LYP/6-311G(d) basis set employing the DFT method to predict comprehensive information in terms of molecular structure and frontier molecular orbitals of the best three compounds identified with the highest energy total among the investigated ones, respectively (Abdelsalam *et al.*, 2019; Beegum *et al.*, 2019; Chinnasamy *et al.*, 2020; Panwar and Singh, 2021). Their quantum chemical descriptors (Ionization potential (I), electron affinity (A), chemical hardness (η), softness (δ), electronegativity (χ), chemical potential (μ) and Electrophilicity index (ω)) were derived from their E_{HOMO} and E_{LUMO} energies, respectively (El Kalai *et al.*, 2019; Omoboyowa, 2022).

Pharmacokinetics Feature Evaluation

The modelling and evaluation of the pharmacokinetics (ADME-Toxic and drug-likeness) properties/features of the studied molecules were assessed using the pkCSM (http://structure.bioc.cam.ac.uk/pkcsm) and SWISSADME (http://www.swissadme.ch/index.php) web servers, respectively (Daina *et al.*, 2017; Hadni and Elhallaoui, 2020; Mills, 2006).

Results and Discussion

The binding modes and affinity of the investigated derivatives of 1-naphthol against the human peroxiredoxin 5 target enzyme (PDB ID: 1HD2) were computationally studied using the molecular docking approach. is an endogenous antioxidant enzyme that protects organisms from damage caused by hydrogen peroxide (H_2O_2) and organic hydroperoxides. As depicted in Table 2, the binding energy ranges from -57.35 to -88.98 kcal/mol total energy calculated for the eleven compounds presented as the outcome of the molecular docking. Based on the values of the binding energies, compounds 8, 6, and 11 showed the highest affinity compound as indicated by their lowest total energies of -88.9812, -86.2011, and -84.718 kcal/mol, respectively.

The re-rank scores also supported the order of ranking; compound 6 had the best re-rank score (-71.1374), followed by compound 8 (-70.9257) and compound 11 (-70.6188). Consistently, the pose energies of the three best ligands had also been relatively low (around 56 to 62 kcal/mol). This further indicates that these binding poses could be energetically stable and could indeed be obtained from the real binding mode in 1HD2.

@ 2026 | PUBLISHED BY GJR PUBLICATION, INDIA

Table 2: Docking energy parameters for the reported 1-naphthol derivatives with 1HD2 protein

Compound ID	Energy -Total	Pose Energy	Re-rank Score
1	-69.6958	-57.7808	-57.4
2	-75.8402	-58.7286	-65.2861
3	-64.2419	-57.5018	-55.2661
4	-68.0924	-56.2721	-54.727
5	-57.3467	-59.8519	-56.1339
6	-86.2011	-61.8582	-71.1374
7	-70.2846	-57.9087	-57.7364
8	-88.9812	-61.2028	-70.9257
9	-71.3021	-56.2237	-58.006
10	-74.7812	-58.0022	-59.93
11	-84.718	-58.0089	-70.6188

The 2D interaction map (Figure 1) and the data in Table 3 show that compound 6 forms two conventional hydrogen bonds with ALA90 (2.62 Å) and GLU9 (2.07 Å). These short-distance hydrogen bonds are expected to contribute substantially to binding affinity. In addition, hydrophobic contacts of the alkyl and π-alkyl types were observed with ARG86 (two interactions), ALA90, and LEU96. The combination of polar hydrogen-bonding and non-polar hydrophobic interactions stabilizes the ligand within a predominantly hydrophobic pocket while still allowing specific polar recognition.

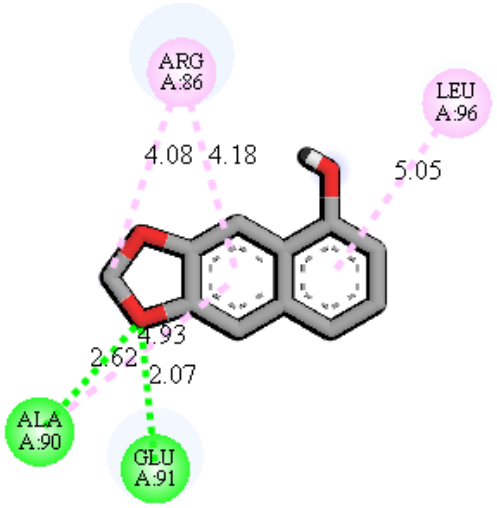

Figure 1: 2D interaction of compound 6 in complex with human peroxiredoxin 5 target enzyme

Compound 8, which had the lowest total energy, formed typical hydrogen bonds with ARG86 (2.71) and ALA90 (2.76). There was a denser network of hydrophobic interactions with the compound, including alkyl and -alkyl interactions from ARG86 (three), ALA90 (three), and LEU96. As indicated in Figure 4, due to the additional hydrophobic interactions in compound 8 compared with compound 6, a slightly lower total energy was observed. The binding pose for each compound was successfully occupied and was similar to the catalytic region of peroxiredoxin 5.

@ 2026 | PUBLISHED BY GJR PUBLICATION, INDIA

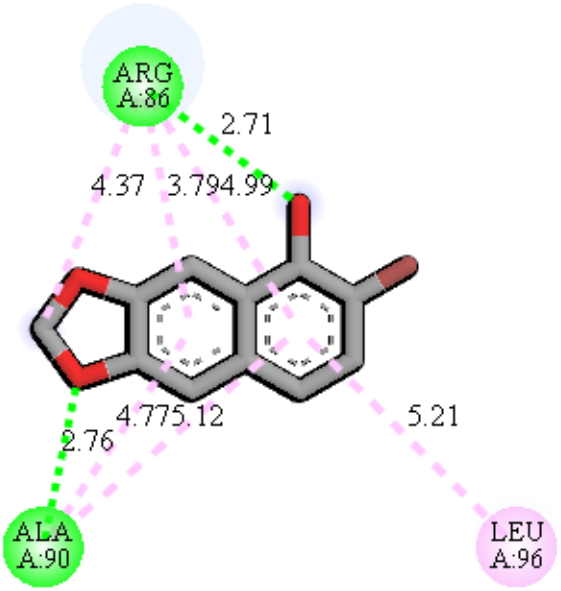

Figure 2: 2D interaction of compound 8 in complex with human peroxiredoxin 5 target enzyme

Compound 11 displayed a richer interaction profile. Two conventional hydrogen bonds were formed with LYS93 (2.38 Å) and VAL94 (1.64 Å)—the latter being particularly short and therefore strong. An additional carbon–hydrogen bond with GLY92 (3.26 Å) and a π–anion electrostatic interaction with GLU16 (3.85 Å) further diversified the binding repertoire. Hydrophobic contacts included π–sigma, alkyl, and π–alkyl interactions with ARG95, ALA90, ARG86, and LEU96. The presence of both electrostatic and hydrogen-bonding interactions, together with extensive hydrophobic contacts, explains the still-high binding affinity of this larger ligand (MW 362.01).

The docking procedure validation was executed by docking compound 8 into the binding pose of the human peroxiredoxin 5 target enzyme, and the root mean square deviation (RMSD) value of the re-docked compound in the active site of the human peroxiredoxin 5 target enzyme was noted as 0.234Å, respectively. The 3D superimposition of compound 8 into the binding pose of the human peroxiredoxin 5 target is depicted in Figure 4.

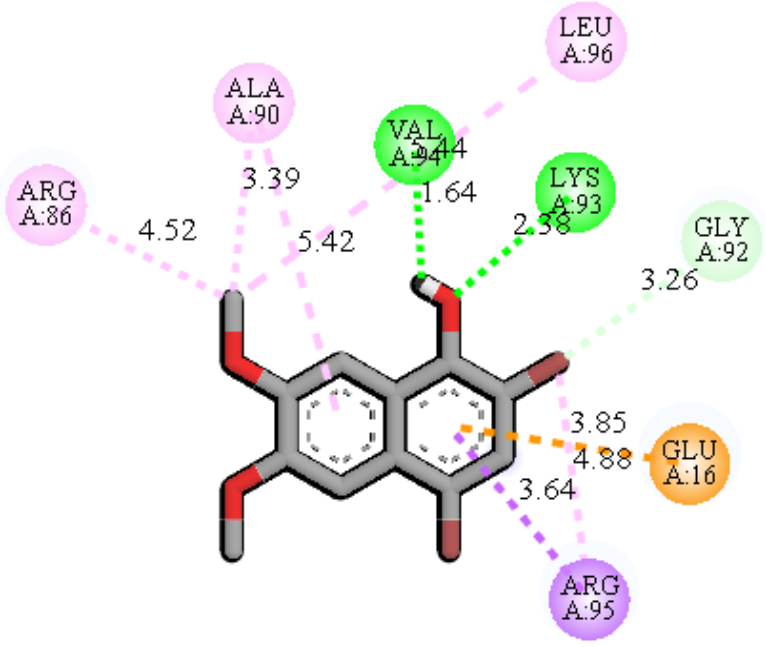

Figure 3: 2D interaction of compound 11 in complex with human peroxiredoxin 5 target enzyme

@ 2026 | PUBLISHED BY GJR PUBLICATION, INDIA

Collectively, the docking results indicate that the most active compounds engage a common set of residues (ALA90, ARG86, LEU96) while also exploiting compound-specific polar contacts. This dual strategy of conserved hydrophobic anchoring and variable polar recognition is characteristic of high-affinity ligands for peroxiredoxin-family enzymes and supports the hypothesis that these 1-naphthol derivatives can modulate the antioxidant function of the target.

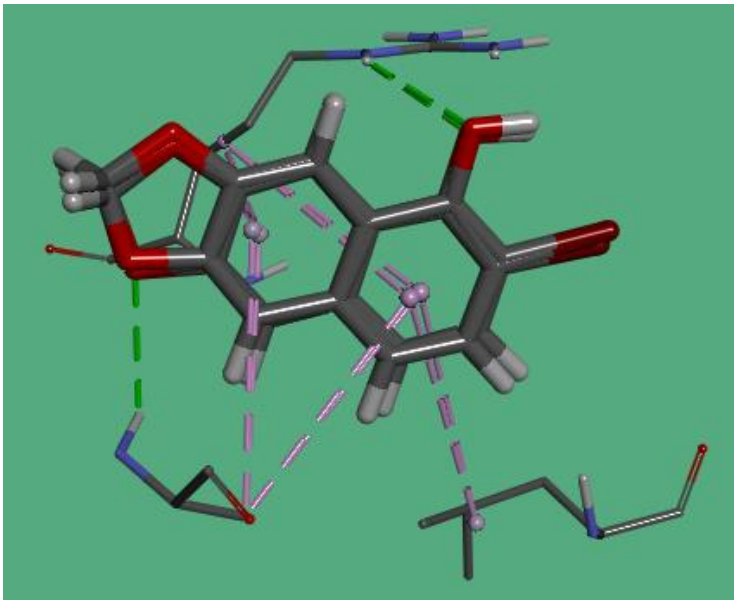

Figure 4: 3D superimposition of compound 8 into the binding pose of the human peroxiredoxin 5 target

Free Radical Scavenging Mechanisms

To rationalize the antioxidant activity at the molecular level, three principal free-radical scavenging pathways were examined thermodynamically in the gas phase: hydrogen-atom transfer (HAT), single-electron transfer followed by proton transfer (SET-PT), and sequential proton-loss electron transfer (SPLET). The key descriptors—bond dissociation enthalpy (BDE), ionization potential (IP), proton dissociation enthalpy (PDE), proton affinity (PA), and electron-transfer enthalpy (ETE)are reported in Table 3.

Hydrogen-Atom Transfer (HAT) Pathway

The HAT mechanism is governed by the BDE of the labile O–H bond. Lower BDE values facilitate hydrogen-atom donation to free radicals. The lowest BDE was observed for compound 6 (291.8 kJ/mol) followed by compounds 11 (302.5 kJ/mol) and 8 (304.6 kJ/mol). These values are substantially lower than the typical BDE of phenolic antioxidants (≈ 330–360 kJ mol−1), indicating that all three compounds are thermodynamically competent hydrogen-atom donors. The superior performance of compound 6 in the HAT pathway correlates with its strong docking affinity and suggests that direct H-atom transfer is a viable primary antioxidant mechanism for this scaffold.

SET-PT and SPLET Pathways

In the SET-PT mechanism, the first step is electron transfer (characterized by IP), followed by proton transfer (PDE). The sum IP + PDE therefore represents the overall energetic cost. Compounds 6, 8, and 11 displayed IP + PDE values of 384.42, 387.48, and 386.98 kJ mol^{-1}, respectively remarkably similar and relatively low. The SPLET pathway proceeds via sequential proton loss (PA) and electron transfer (ETE); the corresponding sums PA + ETE are numerically identical to the IP + PDE values, reflecting thermodynamic equivalence of the two multi-step routes under the computational conditions employed.

Comparison of the three pathways reveals that the HAT mechanism is energetically preferred for all three compounds, as the BDE values (291 - 305 kJ mol^{-1}) are substantially lower than the IP + PDE or PA + ETE sums (≈ 384 - 387 kJ mol^{-1}). Consequently, under gas-phase conditions, the compounds are predicted to act predominantly as hydrogen-atom donors rather than as electron or proton donors. This mechanistic preference is consistent with the classical behavior of phenolic antioxidants and reinforces the design rationale of the 1-naphthol scaffold.

@ 2026 | PUBLISHED BY GJR PUBLICATION, INDIA

Table 3: Thermodynamic Parameters

Compound	Thermodynamic parameters in Gas Phase (kJ/mol)						
	HAT	SET-PT			SPLET		
	BDE	IP	PDE	IP+PDE	PA	ETE	PA+ETE
6	291.8	536.3	1072.1	384.42	1219.8	388.7	384.42
8	304.6	552	1069.3	387.48	1208.7	412.6	387.48
11	302.5	549.5	1069.6	386.98	1194.9	424.2	386.98

HAT: hydrogen atom Transfer Mechanism, SET-PT: single-electron transfer followed by Proton Transfer Mechanism and SPLET: sequential proton-loss electron transfer mechanism.

DFT and Quantum Chemical Calculation

The electronic origin of antioxidant activity is further explained by global reactivity descriptors from density-functional theory (DFT) calculations (Table 4). The HOMO energies of compounds 6, 8 and 11 were -770.66, -766.59 and -777.70 kJ mol^{-1}, respectively, and the corresponding LUMO energies were -455.45, -453.08 and -470.41 kJ mol^{-1}. The HOMO–LUMO band gaps were 315.22 kJ mol^{-1} (compound 6), 313.51 kJ mol^{-1} (compound 8), and 307.29 kJ mol^{-1} (compound 11). The narrower gap of compound 11 implies higher polarizability and greater ease of electronic excitation, which can facilitate electron-transfer processes even though the HAT pathway remains dominant.

Chemical hardness (η) values decreased in the order 6 > 8 > 11 (157.61, 156.76, 153.64 kJ mol−1), confirming that compound 11 is the softest and therefore the most reactive toward soft electrophiles such as free radicals. Electronegativity (χ) and chemical potential (μ) followed the same trend, indicating that compound 11 is the most electron-donating of the three. These electronic properties align with the observed docking affinities and thermodynamic descriptors, providing a coherent multilevel picture of structure–activity relationships.

Table 4: DFT and quantum chemical descriptor computation of the reported compounds (kJ/mol)

	E-HOMO	E-LUMO	Band gap	I	A	η	δ	χ	μ
6	-770.66	-455.45	315.22	770.66	455.45	157.61	0.01	-157.61	157.61
8	-766.59	-453.08	313.51	766.59	453.08	156.76	0.01	-156.76	156.76
11	-777.70	-470.41	307.29	777.70	470.41	153.64	0.01	-153.64	153.64

Pharmacokinetics and Drug-Likeness Feature Evaluation

Drug-likeness and ADME-Tox profiles were assessed to determine the translational potential of the top compounds (Tables 5 and 6). All three molecules satisfy Lipinski's rule of five with zero violations: molecular weights range from 188.18 to 362.01 Da, the number of hydrogen-bond acceptors is three, the number of donors is one, and MLOGP values lie between 1.58 and 3.17. The bioavailability score of 0.55 for each compound indicates a high probability of oral absorption. The compounds are easy to synthesize, as shown by their synthetic accessibility scores, which range between 2.21 and 2.41.

Table 5: Drug-like properties of the reported compounds

Molecule	MW	No H-bond acceptors	No H-bond donors	MLOGP	No of Lipinski violations	Bioavailability Score	Synthetic Accessibility
Molecule 6	188.18	3	1	1.58	0	0.55	2.3
Molecule 8	267.08	3	1	2.26	0	0.55	2.41
Molecule 11	362.01	3	1	3.17	0	0.55	2.21

Absorption, Distribution, Metabolism, Excretion, and Toxicity

Human intestinal absorption was predicted to be excellent for all three ligands (91.7 to 93.3 %). Blood–brain barrier (BBB) permeability values were moderate for compounds 6 and 8 (0.445 and 0.46) and lower for compound 11 (0.086), suggesting that the larger molecule is less likely to cross the BBB, an advantage if central nervous system side effects are to be avoided. CNS permeability values were correspondingly low (≈ -1.7 to -1.9).

@ 2026 | PUBLISHED BY GJR PUBLICATION, INDIA

Metabolically, none of the compounds is predicted to be a CYP2D6 substrate, yet all are CYP3A4 substrates. They inhibit CYP1A2 and, in the cases of compounds 8 and 11, also CYP2C19; they do not inhibit CYP2C9, CYP2D6, or CYP3A4. This selective inhibition profile reduces the risk of broad drug–drug interactions while still requiring attention to CYP1A2- and CYP2C19-mediated pathways. Total clearance values were low to moderate (0.095, −0.033, and 0.339), consistent with reasonable systemic exposure.

Importantly, none of the three compounds was predicted to be hepatotoxic. These 1-naphthol derivatives are promising candidates for prospective preclinical investigation as antioxidant agents due to their low hepatotoxicity risk and excellent absorption and drug-likeness profiles.

Integrated Interpretation and Implications

The present chemoinformatic study integrates molecular docking, thermodynamic analysis of radical-scavenging pathways, quantum-chemical descriptors, and ADME-Tox prediction to construct a coherent structure–activity narrative for a series of 1-naphthol derivatives. Compounds 6, 8, and 11 consistently rank among the best performers across orthogonal computational endpoints. Their strong binding to human peroxiredoxin 5, low BDE values favoring the HAT mechanism, favorable electronic properties, and excellent drug-like profiles collectively suggest that these molecules can both interact productively with a key antioxidant enzyme and act as direct free-radical scavengers.

The HAT route is preferred over SET-PT and SPLET, which is particularly remarkable. It also indicates that the antioxidant activity of these chemicals is usually a lot influenced by the neighboring pH and any optional steel ions that may well increase the electron transfer channels. So, the compounds will most likely maintain their performance across a wide selection of physiological situations. The docking outcomes also recommend that the ligands can defend or control the active site of peroxiredoxin 5, and strengthen the enzyme's innate safety action along with its inbuilt radical-scavenging action. From a medicinal chemistry perspective, the zero Lipinski violations, high predicted intestinal absorption, and absence of hepatotoxicity constitute a strong foundation for lead optimization. Future experimental work should prioritize the synthesis and biological evaluation of compounds 6, 8, and 11, followed by structure–activity relationship studies that systematically vary the substituents responsible for the key hydrogen-bonding and hydrophobic contacts identified herein. In parallel, in-vitro radical-scavenging assays (e.g., DPPH, ABTS, ORAC) and enzyme-inhibition or activation assays against peroxiredoxin 5 will be essential to validate the computational predictions.

Conclusion

An extensive chemoinformatics investigation of 11 1-naphthol derivatives via docking, DFT and pharmacokinetics has identified compounds 6, 8, and 11 as lead molecules for further study. The identified ligands showed the highest affinity (-86.20 to -88.98 kcal mol1) for human peroxiredoxin 5, with significant interactions with ALA90, ARG86, and LEU96 and exhibited promising thermodynamic parameters for hydrogen-atom transfer (HAT; bond-dissociation enthalpy: 291.8 to 304.6 kJ mol1). Density-functional-based descriptors confirmed chemical reactivity, and ADME-Tox predictions established full compliance with the Lipinski rule of five, high predicted intestinal absorption, and no predicted hepatotoxicity. Overall, the computational results strongly support the availability of synthesizable 1-naphthol derivatives with appropriate interactions at the target site, favorable antioxidant thermodynamics, and pharmacokinetics profiles.

Table 6: ADME-toxicity of the reported compounds

Index	Absorption	Distribution		Metabolism							Excretion	Toxicity
	Intestinal absorption	Permeability		Substrate		Inhibitor					Total Clearance	Hepato-toxicity
	human	BBB	CNS	CYP2D6	CYP3A4	CYP1A2	CYP2C19	CYP2C9	CYP2D6	CYP3A4		
6	93.299	0.445	-1.93	No	Yes	Yes	No	No	No	No	0.095	No
8	92.713	0.46	-1.688	No	Yes	Yes	Yes	No	No	No	-0.033	No
11	91.735	0.086	-1.689	No	Yes	Yes	Yes	No	No	No	0.339	No

Acknowledgments

The authors sincerely acknowledge the Tertiary Education Trust Fund (Tetfund) for sponsoring this research under the Tetfund IBR research project grant. M.T. Ibrahim also acknowledged Ahmadu Bello University, Zaria, for their technical support during the course of this research. U. Muhammad also acknowledged Kano State Polytechnic, Kano State technical support during the course of this research.

@ 2026 | PUBLISHED BY GJR PUBLICATION, INDIA

References

1. Abdelsalam, E. A., Zaghary, W. A., Amin, K. M., Abou Taleb, N. A., Mekawey, A. A., Eldehna, W. M., . . . Hammad, S. F. (2019). Synthesis and in vitro anticancer evaluation of some fused indazoles, quinazolines and quinolines as potential EGFR inhibitors. *Bioorganic Chemistry, 89*, 102985.
2. Abdullahi, M., Uzairu, A., Shallangwa, G. A., Arthur, D. E., Umar, B. A., & Ibrahim, M. T. (2020). Virtual molecular docking study of some novel carboxamide series as new anti-tubercular agents. *European Journal of Chemistry, 11*(1), 30-36.
3. Amić, A., Lučić, B., Stepanić, V., Marković, Z., Marković, S., Marković, J. M. D., & Amić, D. (2017). Free radical scavenging potency of quercetin catecholic colonic metabolites: Thermodynamics of 2H+/2e− processes. *Food chemistry, 218*, 144-151.
4. Amić, A., Marković, Z., Klein, E., Marković, J. M. D., & Milenković, D. (2018). Theoretical study of the thermodynamics of the mechanisms underlying antiradical activity of cinnamic acid derivatives. *Food chemistry, 246*, 481-489.
5. Bartmess, J. E. (1994). Thermodynamics of the electron and the proton. *The Journal of Physical Chemistry, 98*(25), 6420-6424.
6. Beegum, S., Panicker, C. Y., Armaković, S., Armaković, S. J., Arisoy, M., Temiz-Arpaci, O., & Van Alsenoy, C. (2019). Spectroscopic, antimicrobial and computational study of novel benzoxazole derivative. *Journal of Molecular Structure, 1176*, 881-894.
7. Bizarro, M. M., Cabral, B. C., Dos Santos, R. B., & Simões, J. M. (1999). Substituent effects on the O–H bond dissociation enthalpies in phenolic compounds: agreements and controversies+ erratum. *Pure and Applied Chemistry, 71*(7), 1249-1256.
8. Chandimali, N., Bak, S. G., Park, E. H., Lim, H.-J., Won, Y.-S., Kim, E.-K., . . . Lee, S. J. (2025). Free radicals and their impact on health and antioxidant defenses: A review. *Cell death discovery, 11*(1), 19.
9. Chinnasamy, S., Selvaraj, G., Kaushik, A. C., Kaliamurthi, S., Chandrabose, S., Singh, S. K., . . . Wei, D.-Q. (2020). Molecular docking and molecular dynamics simulation studies to identify potent AURKA inhibitors: assessing the performance of density functional theory, MM-GBSA and mass action kinetics calculations. *Journal of Biomolecular Structure and Dynamics, 38*(14), 4325-4335.
10. Daina, A., Michielin, O., & Zoete, V. (2017). SwissADME: a free web tool to evaluate pharmacokinetics, drug-likeness and medicinal chemistry friendliness of small molecules. *Scientific reports, 7*, 42717.
11. Dincel, E. D., Gürsoy, E., Yilmaz-Ozden, T., & Ulusoy-Güzeldemirci, N. (2020). Antioxidant activity of novel imidazo [2, 1-b] thiazole derivatives: Design, synthesis, biological evaluation, molecular docking study and in silico ADME prediction. *Bioorganic Chemistry, 103*, 104220.
12. El Kalai, F., Chelfi, T., Benchat, N., Hacht, B., Bouklah, M., Elaatiaoui, A., . . . Almalki, F. (2019). New organic extractant based on pyridazinone scaffold compounds: Liquid-liquid extraction study and DFT calculations. *Journal of Molecular Structure, 1191*, 24-31.
13. Erdoğan, M., Polat Köse, L., Eşsiz, S., & Gülçin, İ. (2021). Synthesis and biological evaluation of some 1-naphthol derivatives as antioxidants, acetylcholinesterase, and carbonic anhydrase inhibitors. *Archiv der Pharmazie, 354*(8), 2100113.
14. Ghamali, M., Chtita, S., Hmamouchi, R., Adad, A., Bouachrine, M., & Lakhlifi, T. (2016). The inhibitory activity of aldose reductase of flavonoid compounds: Combining DFT and QSAR calculations. *Journal of Taibah University for Science, 10*(4), 534-542.
15. Hadni, H., & Elhallaoui, M. (2020). 3D-QSAR, docking and ADMET properties of aurone analogues as antimalarial agents. *Heliyon, 6*(4), e03580.
16. Ibrahim, M. T., Darma, M. S., & Uba, S. (2025). Utilizing computational chemistry to unravel the molecular mechanisms of cystic fibrosis mutations and develop targeted therapeutics. *Journal of Physical Chemistry and Functional Materials, 8*(2), 56-68.
17. Ibrahim, M. T., Uzairu, A., Shallangwa, G. A., & Uba, S. (2020). Structure-based design and activity modeling of novel epidermal growth factor receptor kinase inhibitors; an in silico approach. *Scientific African*, e00503.
18. Jomova, K., Raptova, R., Alomar, S. Y., Alwasel, S. H., Nepovimova, E., Kuca, K., & Valko, M. (2023). Reactive oxygen species, toxicity, oxidative stress, and antioxidants: chronic diseases and aging. *Archives of toxicology, 97*(10), 2499-2574.
19. Khodja, I. A., Boulebd, H., Bensouici, C., & Belfaitah, A. (2020). Design, synthesis, biological evaluation, molecular docking, DFT calculations and in silico ADME analysis of (benz) imidazole-hydrazone derivatives as promising antioxidant, antifungal, and anti-acetylcholinesterase agents. *Journal of Molecular Structure, 1218*, 128527.
20. Klein, E., Rimarcik, J., & Lukes, V. (2009). DFT/B3LYP study of the O–H bond dissociation enthalpies and proton affinities of para-and meta-substituted phenols in water and benzene. *Acta Chim. Slovaca, 2*(2), 37-51.
21. Kohn, W., Becke, A. D., & Parr, R. G. (1996). Density functional theory of electronic structure. *The Journal of Physical Chemistry, 100*(31), 12974-12980.

@ 2026 | PUBLISHED BY GJR PUBLICATION, INDIA

22. Mills, N. (2006). ChemDraw Ultra 10.0 CambridgeSoft, 100 CambridgePark Drive, Cambridge, MA 02140. www. cambridgesoft. com. Commercial Price: 1910fordownload, 2150 for CD-ROM; Academic Price: 710fordownload, 800 for CD-ROM. In: ACS Publications.
23. Omoboyowa, D. A. (2022). Virtual Screening of Phyto-compounds from Blighia sapida as Protein Tyrosine Phosphatase 1B Inhibitor: A Computational Approach Against Diabetes. *Chemistry Africa*, 1-11.
24. Panwar, U., & Singh, S. K. (2021). Atom-based 3D-QSAR, molecular docking, DFT, and simulation studies of acylhydrazone, hydrazine, and diazene derivatives as IN-LEDGF/p75 inhibitors. *Structural Chemistry, 32*(1), 337-352.
25. Parker, V. D. (1992). Homolytic bond (HA) dissociation free energies in solution. Applications of the standard potential of the (H+/H. bul.) couple. *Journal of the American Chemical Society, 114*(19), 7458-7462.
26. Patlevič, P., Vašková, J., Švorc Jr, P., Vaško, L., & Švorc, P. (2016). Reactive oxygen species and antioxidant defense in human gastrointestinal diseases. *Integrative medicine research, 5*(4), 250-258.
27. Pawara, R., Ahmad, I., Surana, S., & Patel, H. (2021). Computational identification of 2, 4-disubstituted amino-pyrimidines as L858R/T790M-EGFR double mutant inhibitors using pharmacophore mapping, molecular docking, binding free energy calculation, DFT study and molecular dynamic simulation. *In Silico Pharmacology, 9*(1), 1-22.
28. Reddy, V. P. (2023). Oxidative stress in health and disease. *Biomedicines, 11*(11), 2925.
29. Sotler, R., Poljšak, B., Dahmane, R., Jukić, T., Pavan Jukić, D., Rotim, C., . . . Starc, A. (2019). Prooxidant activities of antioxidants and their impact on health. *Acta Clinica Croatica, 58*(4.), 726-736.
30. Wu, X., Beecher, G. R., Holden, J. M., Haytowitz, D. B., Gebhardt, S. E., & Prior, R. L. (2004). Lipophilic and hydrophilic antioxidant capacities of common foods in the United States. *Journal of agricultural and food chemistry, 52*(12), 4026-4037.

CITATION

Muhammad, U., & Ibrahim, M. T. (2026). A chemo-informatics Strategy to Understand the Mode of Binding Interaction, Mechanism of Free Radical Scavenging, and Pharmacokinetic Profile of some Antioxidant Agents. Global Journal of Research in Agriculture & Life Sciences, 6(6), 15–25. https://doi.org/10.5281/zenodo.24158303

@ 2026 | PUBLISHED BY GJR PUBLICATION, INDIA